Supporting Information: Controlling Hydrogen Evolution Reaction Activity by Tuning the Size of Pt Islands on Amorphous Ni Cores

Ali Alinezhad,[a] Tania M. Benedetti,[a] Jiaxin Lian,[a] Vinicius R Gonçales,[a] Justin Gooding,[a,b,c] Richard D. Tilley*[a,c,d]

a. School of Chemistry, University of New South Wales, Sydney, NSW 2052 (Australia).
b. Australian Centre for Nanomedicine, University of New South Wales, Sydney, NSW, 2052 (Australia)
c. ARC Centre of Excellence in Convergent Bio-Nano Science and Technology, University of New South Wales, Sydney, NSW, 2052 (Australia)
d Electron Microscope Unit, Mark Wainwright Analytical Centre, University of New South Wales Sydney, NSW 2052 (Australia)

Corresponding Author
*r.tilley@unsw.edu.au

Contents

Materials and methods

Synthesis of amorphous Nickel seeds: A solution was made up with nickel (II) acetylacetonate (86 mg, Acros, 96%), hexadecylamine (765mg, Aldrich, 98%) and trioctylphosphine (60 µL; Aldrich, 97%) dissolved in 5 mL mesitylene in a 21 mL vial. The solution was then transferred to a Fischer-Porter bottle which was degassed under vacuum and filled to 1 bar with hydrogen. The Fischer-Porter bottle was placed into the oven which was at 140°C and left to react for 24 hours. After the reaction Ni nanoparticles transferred to the glovebox and stored in 10 mL degassed toluene.

Synthesis of Ni–Pt islands nanoparticles: For Ni-1.5 nm Pt islands platinum acetylacetonate (10 mg, 0.036 mmol Aldrich, 97%) dissolved in toluene were added to diluted Ni seeds (1 mL, 0.03 mmol) and transferred to a Fischer-Porter bottle in the glove box. The Fisher-Porter bottle was removed from the glovebox and then filled with 3 bar hydrogen before placing it in an oven at 40°C. After 24 h, the bottle was removed from the oven and cooled to room temperature. The gas was released, and the solution was transferred to a vial and cleaned twice by placing magnet beside the vial followed by redispersion in toluene

For Ni-Pt nanoparticles with 2, 2.6 and 3.8 nm Pt islands the identical procedure was performed except reaction temperature was changed to 50, 60 and 70°C, respectively. During the coating synthesis, using air-free techniques (to prevent Ni form oxidation) was essential for direct growth of Pt atoms on Ni.

Characterisation

Low-resolution TEM images and EDX spectrum were taken by Philips CM 200 electron microscopy. High-resolution TEM, selected area electron diffraction pattern (SAED), and EDX mapping were performed on a JEOL JEM-F200 FEG transmission electron microscope operated at 200 kV. This microscope is equipped with a 2k x 2k CCD camera, ADF and BF detectors for STEM imaging and a windowless 100 mm2 SDD EDX detector. EDX results were analysed using the Pathfinder software and the data presented has been filtered to remove background counts and Bremsstrahlung radiation. In all cases, TEM samples were prepared by diluting the samples in hexane and dropping the liquid sample onto carbon-coated copper grids. Inductively coupled plasma optical emission spectroscopy (ICP-OES) analysis was performed on an Optima7300DV- ICP-OES Perkin Elmer instrument.

Electrochemical studies

To prepare catalysts, synthesized nanoparticles were loaded on carbon support (Vulcan XC-72R) by dispersing surfactant stabilized nanoparticles and carbon in hexane (Aldrich) under ultrasonication for 2 h. The carbon loaded nanoparticles were precipitated by centrifugation at 4000 rpm for 10 min. After drying, surfactant was removed by placing carbon loaded nanoparticles in a tube furnace at 220 °C for 5 h under airflow. Commercial Pt/C (PK catalyst) catalyst 5 wt% was used as a reference. Catalyst inks were prepared by dispersing 2.5 mg of the carbon-supported particles in 1 mL of a mixture of deionized water, isopropanol and Nafion (Aldrich 5 vol %) with 75, 24.6 and 0.4 vol%, respectively, by ultrasonication until a uniform ink was obtained. An aliquot of 20 µL of the ink was deposited on a glassy-carbon rotating disk electrode (0.196 cm^2, Autolab) and dried at 120 °C in the oven for 3 min to form a uniform thin film as the working electrode. The electrochemical measurements were performed on an µAutolab III potentiostat using a three-electrode cell setup.

An Hg/HgO (1 mol L^{-1} NaOH) was used as the reference electrode, and a platinum mesh as the counter electrode. A solution of 0.1 mol L^{-1} KOH prepared with deionized water was used as the electrolyte. Prior to each test, the exact pH of the solution was measured with a pH meter.

All the potentials are given relative to the reversible hydrogen electrode (RHE) by measuring the potential difference between the reference electrode and a freshly prepared SHE prior the experiments and considering the electrolyte pH accordingly to the Nernst equation:

$$E_{RHE} = measured\ E_{Hg/HgO} + difference\ measured\ against\ SHE + 0.0591\ x\ pH \quad \text{Eq. S1}$$

The HER activity of catalysts was measured under rotation of the RDE at 1600 rpm in a 0.1 mol L^{-1} KOH solution saturated with Ar gas. The potential was scanned from 0.1 to -0.4 V (vs RHE) in the cathodic direction with the scan rate of 10 mV s^{-1}. All polarization curves were subtracted by the capacitive current curve to obtain HER curves. Prior to electrochemical measurements, catalysts were electrochemically activated by running 20 potentiodynamic cycles between 0 and 1.7 V vs RHE with a scan rate of 200 mV s^{-1} in N_2-saturated 0.1 M KOH. The. 0.1 mol L^{-1} KOH was chosen rather than (1 mol L^{-1}) to decrease the effect of K^+ on HER and lessen the pH error.[2]

The electrochemical surface area (ECSA) of the catalysts were obtained by integrating the area of the CO stripping peak in the first cycle subtracted from second cycle in the potential window of 0.35-.1 V. The CO stripping was performed by holding the electrode potential at 0.1 V vs RHE for 10 min in 0.1 M KOH bubbling with CO to obtain a full monolayer of adsorbed CO on the surface and then switching to flow Ar for another 10 min to remove dissolved CO in the electrolyte, followed by scanning the potential from 0 to 1.7 V vs RHE at a scan rate of 200 mV s^{-1}. The 420 μC cm^{-2} relationship was used to determine the ECSA.

The accurate amount of the Pt loading in each sample was quantified by using inductively-couple plasma mass spectroscopy (ICP-MS), which is listed in Table S1. The specific activity and mass activity were calculated by dividing the HER current at a given potential by the ECSA and the total mass of Pt for each catalyst, respectively. Measurements for all the samples were repeated at least three times to get the average values.

The stability tests were performed by chronopotentiometry at 10 mA cm^{-2} considering the ECSA of the different samples for 6 h in N_2-saturated electrolyte while the working electrode was rotating at speed of 500 rpm to get rid of produced hydrogen bubbles

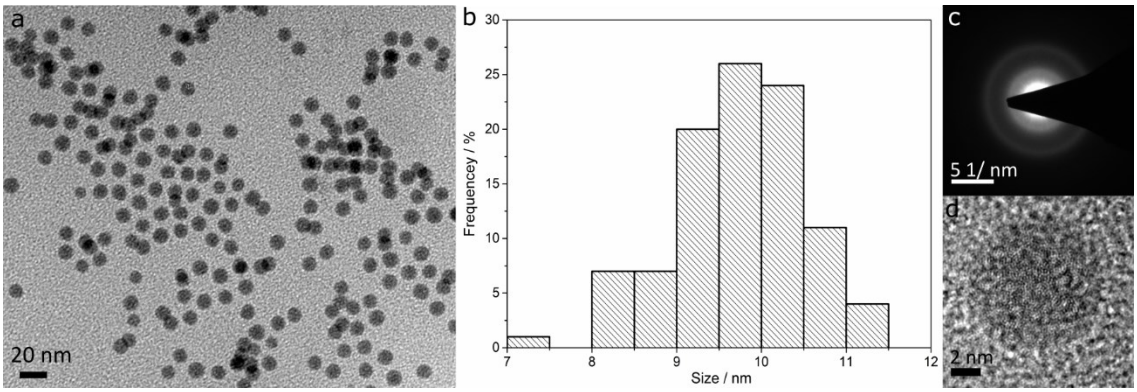

Fig. S1. a) TEM image and b) size distribution of Ni nanoparticles used as seeds. c) Electron diffraction and d) High-resolution TEM image of Ni nanoparticles showing the amorphous nature of these particles

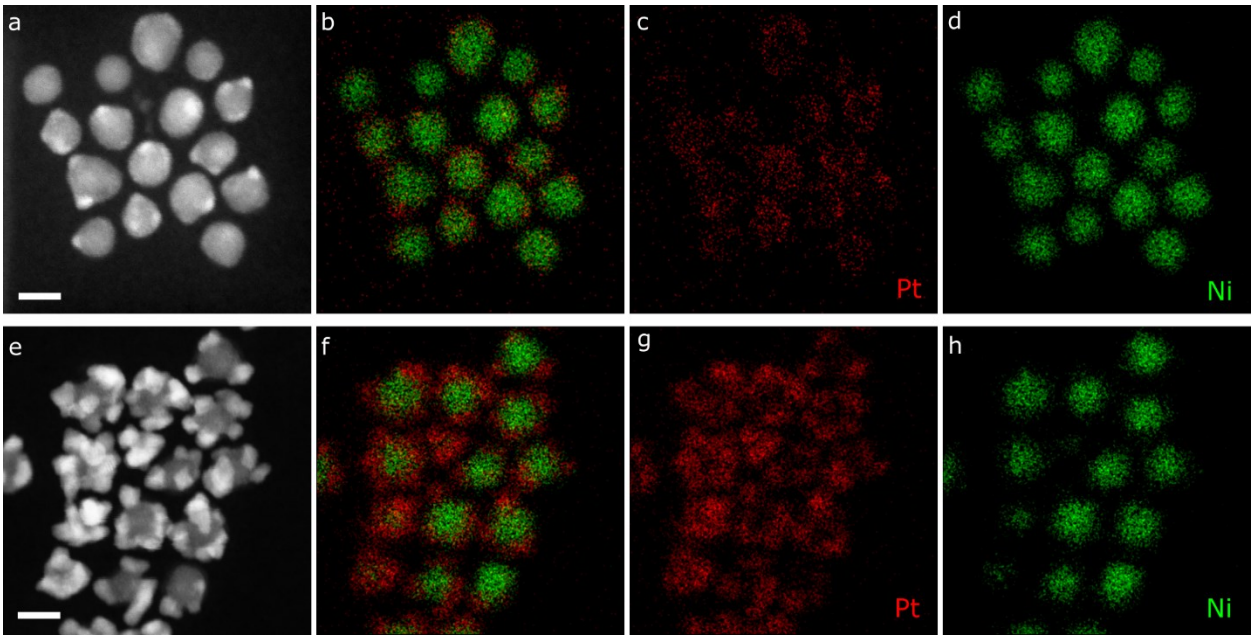

Fig. S2. HAADF-STEM images and STEM-EDX maps of the Ni-Pt island nanoparticles: a-d) 1.5 nm Pt islands and e-h) 3.8 nm Pt islands, showing the formation of larger islands covering a higher proportion of the Ni surface. Scale bar is 10 nm.

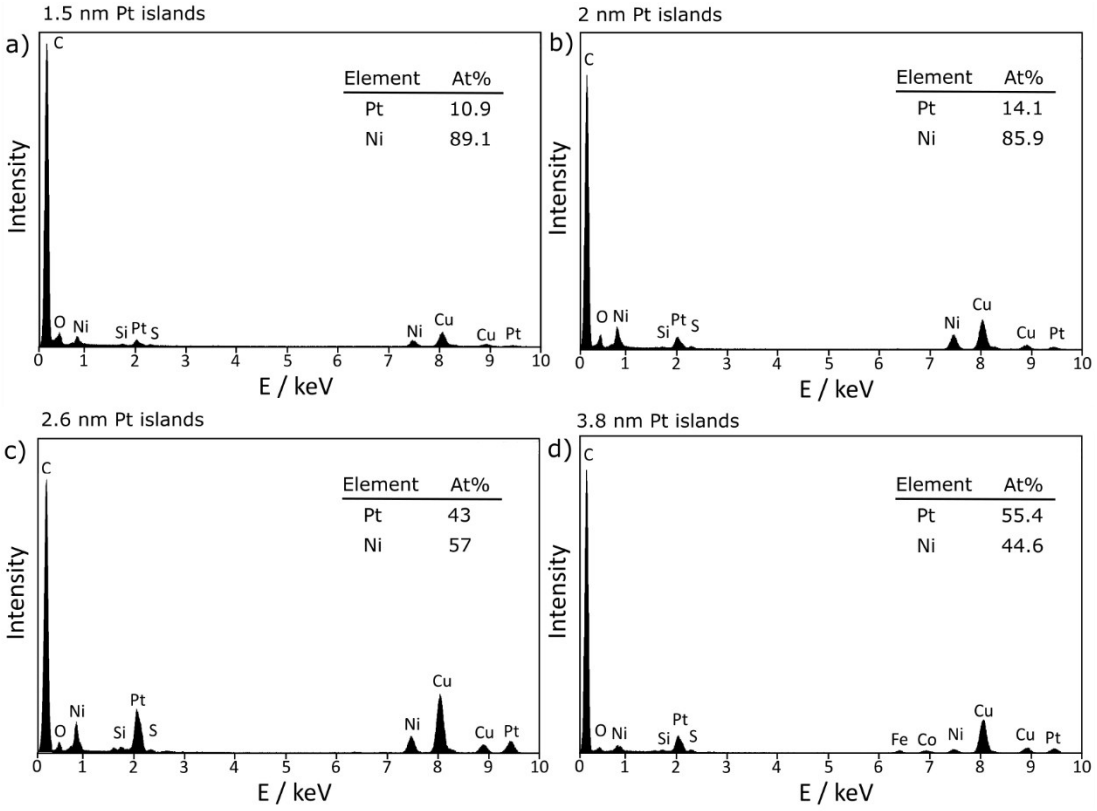

Fig. S3. Typical EDX spectrum of Ni-Pt islands nanoparticles showing the atomic ratio of Pt:Ni.

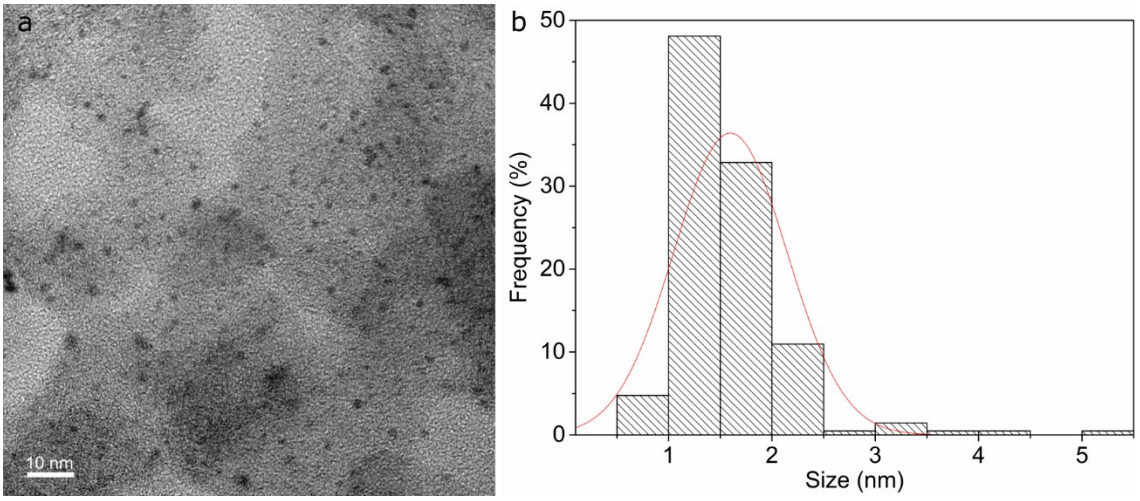

Fig. S4: a) TEM image of commercial Pt nanoparticles and b) histogram of the measured size distribution, 1.6 ± 0.5 nm.

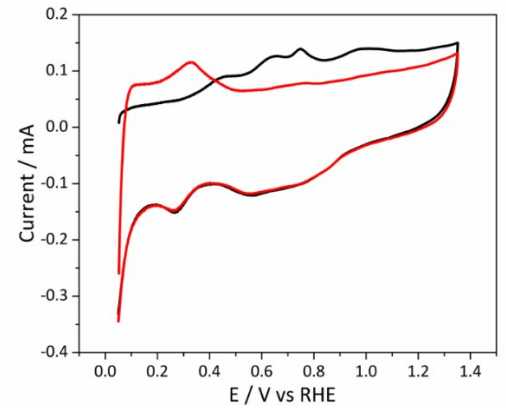

Fig. S5. CO-stripping of commercial Pt nanoparticles in Ar-saturated 0.1 M KOH with a scan rate of 200 mV s^{-1}. The black curve is for the stripping of a monolayer of CO in the first cycle. The red curve is for the following cycle after the CO stripping, representing the CV of the sample.

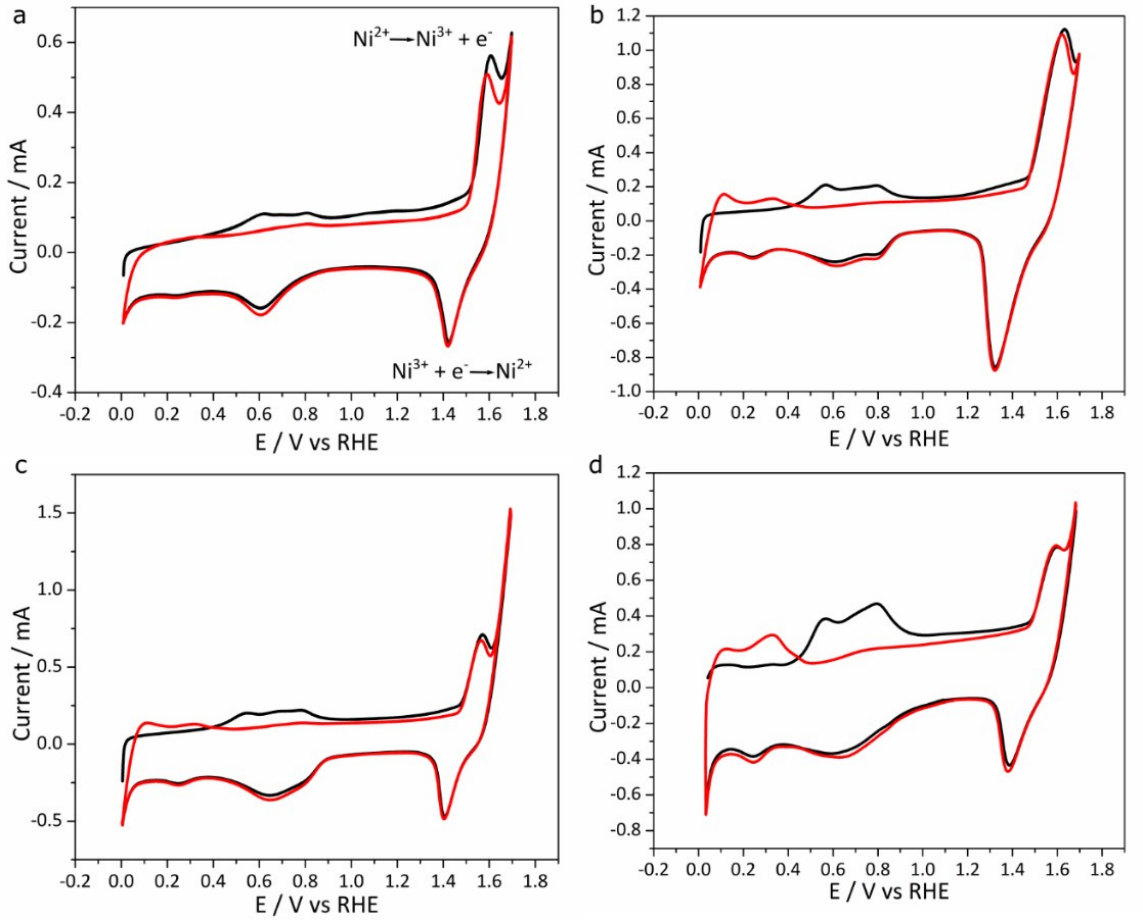

Fig. S6. CO-stripping and corresponding CVs of Ni-Pt island nanoparticles in Ar-saturated 0.1 M KOH with a scan rate of 200 mV s^{-1}: a) 1.5 nm Pt island, b) 2 nm Pt island, c) 2.6 nm Pt island and d) 3.8 nm Pt island nanoparticles. The black curve is for the

stripping of a monolayer of CO in the first cycle. The red curve is for the following cycle after the CO stripping, representing the CV of the sample.

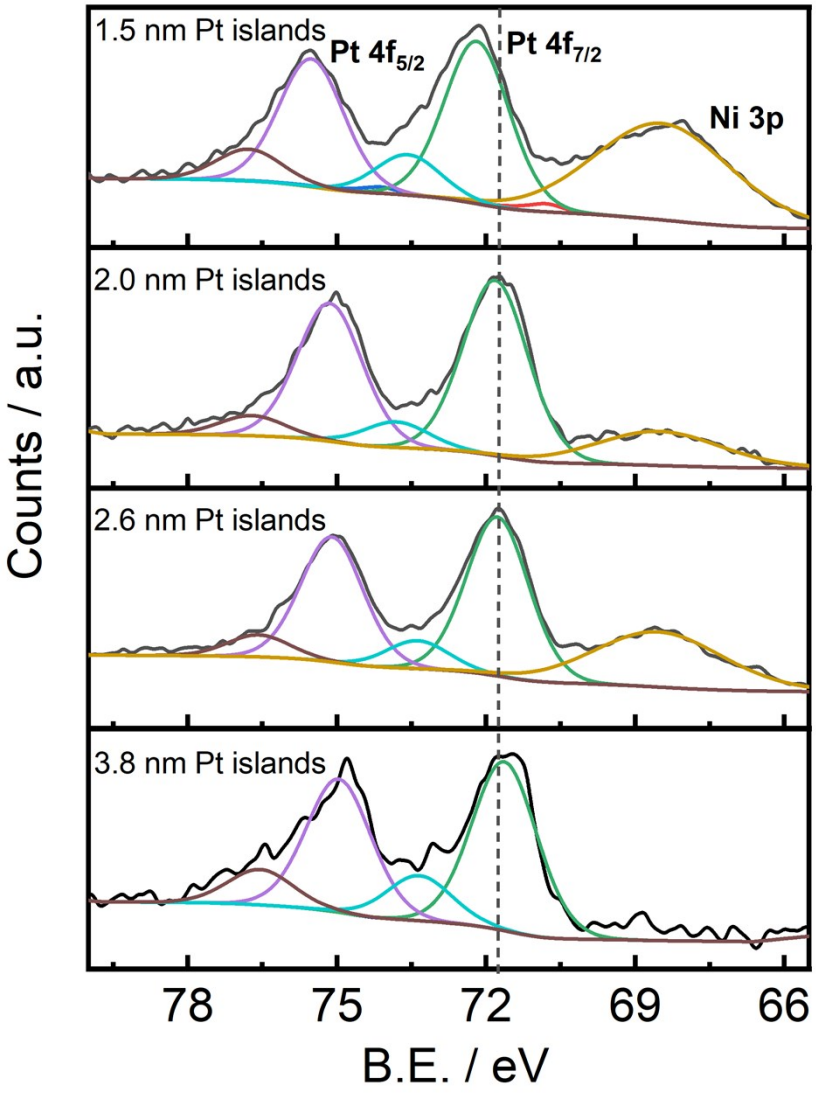

Fig. S7. Pt 4f core-level XPS spectra of Ni-Pt islands catalysts.

Table S1. The percentage of islands in different size ranges for synthesised Ni-Pt islands nanoparticles calculated from Pt islands size histograms.

Sample	islands <1.6 nm	1.6 nm <islands < 2.3 nm	2.3 nm < islands< 3.4 nm	islands> 3.4 nm
1.5 nm Pt islands	61%	37%	2%	0
2 nm Pt islands	18%	54.5%	26.5%	1%
2.6 nm Pt islands	6.5%	39.5%	50%	4%
3.8 nm Pt islands	0	3.5%	31%	65.5%

Table S2. ECSA and Pt loading of different catalysts used in this study.

Sample	ECSA calculated from CO-stripping (cm^2)	Pt loading on carbon calculated from ICP (wt%)	Pt used in ink (µg)
1.5 nm Pt islands	0.08 ± 0.01	0.4	0.2
2 nm Pt islands	0.44 ± 0.01	2.8	1.4
2.6 nm Pt islands	0.40 ± 0.05	2.7	1.3
3.8 nm Pt islands	0.91 ± 0.1	6.5	3.25
Commercial Pt	1 ± 0.1	5	2.5

Table S3. Comparison of HER specific activity of Ni-Pt island catalyst with other high performance HER catalysts in alkaline condition (The current densities in the table are normalized to ECSA of catalyst)

Sample	Specific activity @ -70 mV	Journal, Year	reference
Pt3Ni frames/C	2.3	Science, 2014	[1]
Ni(OH)2/Pt islands/Pt(111)	2.2	Science, 2011	[2]
Ni(OH)2/modified Pt surface	2.7	Angew. Chem. Int. Ed. 2012	[3]
Pt NWs/SL-Ni(OH)2	2.48	Nat. Commun. 2015	[4]
Pt/C/20 wt% SL Ni(OH)2 Li(OH)	2.28	ACS Catal. 2015	[5]
Pt (111)/Co(OH)2	0.5	Nature Materials 2012	[6]
Pt-Co(OH)2/CC	1.52	ACS Catal. 2017	[7]
Ni- 1.5 nm Pt islands	2.8		This work

Table S4. Pt: Ni ratio at the surface of nanoparticles calculated from corresponding curves from CVs in Fig. S7.

Sample	Charge corresponding to Pt calculated from integration of Co stripping peak in the potential range of 0.35-1 V (μC)	Charge corresponding to Ni calculated from integration of Ni^{3+} to Ni^{2+} reduction peak (μC)	Pt:Ni ratio at the surface of nanoparticles obtained from the corresponding charges
1.5 nm Pt island	41	177	0.22
2 nm Pt island	185	610	0.3
2.6 nm Pt island	167	198	0.84
3.8 nm Pt island	384	235	1.62

Since the Ni^{2+} to Ni^{+3} oxidation peak overlaps with OER, the reduction peak (Ni^{3+} to Ni^{2+}) in cathodic direction is used for calculating the charge corresponds to Ni at the surface.

References

1. C. Chen, Y. Kang, Z. Huo, Z. Zhu, W. Huang, H. L. Xin, J. D. Snyder, D. Li, J. A. Herron, M. Mavrikakis, M. Chi, K. L. More, Y. Li, N. M. Markovic, G. A. Somorjai, P. Yang and V. R. Stamenkovic, *Science*, 2014, **343**, 1339-1343.
2. R. Subbaraman, D. Tripkovic, D. Strmcnik, K. C. Chang, M. Uchimura, A. P. Paulikas, V. Stamenkovic and N. M. Markovic, *Science*, 2011, **334**, 1256-1260.
3. N. Danilovic, R. Subbaraman, D. Strmcnik, K.-C. Chang, A. P. Paulikas, V. R. Stamenkovic and N. M. Markovic, *Angew. Chem. Int. Ed.*, 2012, **51**, 12495-12498.
4. H. Yin, S. Zhao, K. Zhao, A. Muqsit, H. Tang, L. Chang, H. Zhao, Y. Gao and Z. Tang, *Nat. Commun.*, 2015, **6**, 6430.
5. L. Wang, C. Lin, D. Huang, J. Chen, L. Jiang, M. Wang, L. Chi, L. Shi and J. Jin, *ACS Catal.*, 2015, **5**, 3801-3806.
6. R. Subbaraman, D. Tripkovic, K.-C. Chang, D. Strmcnik, A. P. Paulikas, P. Hirunsit, M. Chan, J. Greeley, V. Stamenkovic and N. M. Markovic, *Nat. Mater.*, 2012, **11**, 550.
7. Z. Xing, C. Han, D. Wang, Q. Li and X. Yang, *ACS Catal.*, 2017, **7**, 7131-7135.